

# Development and Evaluation of Ensemble Learning-based Environmental Methane Detection and Intensity Prediction Models

Environmental Health Insights  
Volume 18: 1–11  
© The Author(s) 2024  
Article reuse guidelines:  
sagepub.com/journals-permissions  
DOI: 10.1177/11786302241227307



Reek Majumder<sup>1</sup>, Jacquan Pollard<sup>1</sup>, M Sabbir Salek<sup>1</sup>, David Werth<sup>2</sup>, Gurcan Comert<sup>3</sup>, Adrian Gale<sup>3</sup>, Sakib Mahmud Khan<sup>1</sup>, Samuel Darko<sup>4</sup> and Mashrur Chowdhury<sup>1</sup>

<sup>1</sup>Glenn Department of Civil Engineering, Clemson University, Clemson, SC, USA. <sup>2</sup>Savannah River National Laboratory, Aiken, SC, USA. <sup>3</sup>Comp. Sci., Phy., and Engineering Department, Benedict College, Columbia, SC, USA. <sup>4</sup>School of Arts and Sciences, Florida Memorial University, Miami Gardens, FL, USA.

**ABSTRACT:** The environmental impacts of global warming driven by methane (CH<sub>4</sub>) emissions have catalyzed significant research initiatives in developing novel technologies that enable proactive and rapid detection of CH<sub>4</sub>. Several data-driven machine learning (ML) models were tested to determine how well they identified fugitive CH<sub>4</sub> and its related intensity in the affected areas. Various meteorological characteristics, including wind speed, temperature, pressure, relative humidity, water vapor, and heat flux, were included in the simulation. We used the ensemble learning method to determine the best-performing weighted ensemble ML models built upon several weaker lower-layer ML models to (i) detect the presence of CH<sub>4</sub> as a classification problem and (ii) predict the intensity of CH<sub>4</sub> as a regression problem. The classification model performance for CH<sub>4</sub> detection was evaluated using accuracy, F1 score, Matthew's Correlation Coefficient (MCC), and the area under the receiver operating characteristic curve (AUC ROC), with the top-performing model being 97.2%, 0.972, 0.945 and 0.995, respectively. The  $R^2$  score was used to evaluate the regression model performance for CH<sub>4</sub> intensity prediction, with the  $R^2$  score of the best-performing model being 0.858. The ML models developed in this study for fugitive CH<sub>4</sub> detection and intensity prediction can be used with fixed environmental sensors deployed on the ground or with sensors mounted on unmanned aerial vehicles (UAVs) for mobile detection.

**KEYWORDS:** Methane, fugitive CH<sub>4</sub> emissions, autonomous environmental detection, machine learning, cyber-physical system

**RECEIVED:** September 30, 2023. **ACCEPTED:** January 4, 2024.

**TYPE:** Original Research

**FUNDING :** The author(s) disclosed receipt of the following financial support for the research, authorship, and/or publication of this article: This work was supported by the Department of Energy Office of Environmental Management Minority Serving Institutions Partnership Program (MSIPP) managed by the Savannah River National Laboratory under BSRA contract TOA 0000525174 CN1. Any opinions, findings, conclusions, and recommendations expressed in this material are those of the author(s). They do not necessarily reflect the views of the Savannah River National Laboratory and the U.S. Government assumes no liability for the contents or use thereof.

**DECLARATION OF CONFLICTING INTERESTS:** The author(s) declared no potential conflicts of interest with respect to the research, authorship, and/or publication of this article.

**CORRESPONDING AUTHOR:** Reek Majumder, Glenn Department of Civil Engineering, Clemson University, Room 318, Fluor Daniel Engineering Innovation Building, Clemson, SC 29634, USA. Email: rmajumd@clemson.edu

M. Sabbir Salek, One Research Dr, Room #414A, Clemson University International Center for Automotive Research (CU-ICAR), Greenville, SC 29607, USA. Email: msalek@clemson.edu

## Introduction

Methane (CH<sub>4</sub>) emissions have garnered considerable research interest in recent years. Governmental organizations like the Environmental Protection Agency (EPA) have attempted to improve inaccurate estimates of industrial CH<sub>4</sub> leakage.<sup>1</sup> Methane is a powerful greenhouse gas (GHG) that contributes to global warming. Its impact on the environment has been found to possess far greater consequences on global climate systems over shorter periods than other GHGs such as carbon dioxide (CO<sub>2</sub>), nitrous oxide (N<sub>2</sub>O), chlorofluorocarbons (CFC), and others.<sup>2</sup> The significance of this finding is reflected in the global warming potential (GWP), a metric that measures the global warming impact of various GHGs relative to 1 ton of CO<sub>2</sub>. With a GWP of methane 27 to 30 over a 100-year timescale,<sup>3</sup> it is shown that although CH<sub>4</sub> is a short-lived GHG, it is far more efficient at absorbing radiation than CO<sub>2</sub> and contributes significantly to global warming.<sup>4</sup> This finding indicates that methane's propensity for absorbing and trapping radiation in the atmosphere negatively impacts the environment substantially more than CO<sub>2</sub> over a 20-year timeframe.

The largest source of CH<sub>4</sub> emissions in the U.S. is attributed to the energy sector by processes related to the production, extraction, and transportation of fossil fuels.<sup>5</sup> As the primary constituent in natural gas, CH<sub>4</sub> may enter the environment through cracks and fissures in degraded or defective pipeline infrastructure which spans over 2.6 million miles. These pipeline networks deliver 25% of the energy consumed by the U.S. population for various uses, such as fueling automobiles and regulating temperatures inside residential and commercial buildings.<sup>6</sup> However, the traversing of oil and natural gas (ONG) infrastructure through major urban areas compounds the dangers of fugitive CH<sub>4</sub> emissions. Consequently, it raises negative implications for human health and environmental impacts due to CH<sub>4</sub> emissions being devoid of color and odor and possessing a highly volatile nature. The increased focus on CH<sub>4</sub> emissions caused by ONG distribution systems has been motivated by the substantial benefits of employing early detection technologies for CH<sub>4</sub> emissions. Manual measurement methods for the early detection of methane suffer from various limitations. These include limited sampling coverage that may



Creative Commons Non Commercial CC BY-NC: This article is distributed under the terms of the Creative Commons Attribution-NonCommercial 4.0 License (<https://creativecommons.org/licenses/by-nc/4.0/>) which permits non-commercial use, reproduction and distribution of the work without further permission provided the original work is attributed as specified on the SAGE and Open Access pages (<https://us.sagepub.com/en-us/nam/open-access-at-sage>).

not account for localized emissions, delayed detection, a lack of real-time monitoring, and risks to personnel safety. Moreover, the considerable possibility of human error and a lack of data analysis and integration from multiple sensors make it difficult to implement early-warning programs. According to recent studies,<sup>7,8</sup> the average time to perform mitigating procedures for fugitive CH<sub>4</sub> emissions will be significantly reduced by employing large-scale autonomous environmental emission detection systems requiring minimal human involvement.

Statistical methods and data analysis techniques employed by artificial intelligence and machine learning (ML) algorithms provide the ability to extract useful information from complex data-driven analytical tasks. Recent studies conducted in environmental monitoring applications have employed novel approaches using the intelligent decision-making capabilities of ML algorithms to guide the efficient use of limited resources.<sup>8</sup> In an environmental emissions application, ML algorithms can detect the presence of harmful pollutants or contaminants by processing atmospheric meteorological data. A heterogeneous environmental sensor network consisting of fixed and mobile sensors backed by ML can improve environmental surveillance of fugitive CH<sub>4</sub> emissions by being distributed across multiple sensor edges and geographical areas for large-scale detection, mitigation, and reduced operator response times. This paper aims to develop and assess the performance of the ensemble learning model developed with several data-driven ML models to achieve an autonomous and efficient detection of fugitive CH<sub>4</sub> emissions with minimal false alarms.

The rest of this paper is organized as follows: the review of the literature is covered in Section 2. In Section 3, we describe the dataset, data preprocessing steps and ensemble learning models with hyperparameters used in this study. Section 4 discusses the methods used and results obtained for CH<sub>4</sub> environmental emissions in our study. Section 5 concludes this paper and Section 6 presents some remarks for future research initiatives.

## Literature Review

Many studies in the literature have investigated various strategies to implement large-scale environmental monitoring and mitigation of fugitive CH<sub>4</sub> emissions. This section provides a brief discussion of previous research focused on large-scale environmental assessments, and their limitations.

In a comparative review conducted in 2021, Sun et al.,<sup>9</sup> investigated how CH<sub>4</sub> emissions estimation technologies, data analysis, and probabilistic tools for emission uncertainty estimation unite to form an efficient system of CH<sub>4</sub> management for the ONG energy sector. The authors found that spatial scale was a primary factor in selecting CH<sub>4</sub> emission measurement technology where bottom-up or top-down methods were applied to calculate emission rates from CH<sub>4</sub> concentrations. Bu et al.<sup>10</sup> addressed the leakage and diffusion characteristics of

fugitive CH<sub>4</sub> emissions in utility tunnels using a simulation-based approach under various working conditions. They achieved an average error of 8.29% using a methane invasion distance (MID) prediction equation to accurately predict the location of fugitive CH<sub>4</sub> emissions under various leakage times for optimal placement of utility tunnel alarm devices. Fleming et al.<sup>11</sup> conducted a field-based case study that examined CO<sub>2</sub> and CH<sub>4</sub> efflux measurements over 2 weeks around a petroleum well in Alberta, Canada, using automated dynamic closed chambers. The authors concluded that quantifying the efflux rate of CO<sub>2</sub> and CH<sub>4</sub> was challenging due to spatiotemporal emission variability and suggested that spatiotemporal variability must be considered for accurate fugitive CH<sub>4</sub> migration estimations. Bezyk et al.<sup>12</sup> used the static chamber method to investigate the factors inducing CH<sub>4</sub> uptake for 3 different land uses in Wroclaw, Poland. The findings from their study showed that a threshold for soil temperature and moisture in urban environments acts as a sink for fugitive CH<sub>4</sub> emissions. Okorn et al.<sup>13</sup> used innovative sensors to measure gaseous pollutants, such as fugitive CH<sub>4</sub> emissions, CO<sub>2</sub>, carbon monoxide, etc., in 3 different urban areas in Los Angeles. The authors used a multi-sensor linear regression calibration model and achieved an improvement of 16% coefficient of determination and a 22% reduction in the root mean square error.

Hahnel et al.<sup>14</sup> applied a deep learning framework for air pollution monitoring and forecasting to extend model training across different domains, whereas Eldakhly et al.<sup>15</sup> investigated several methods to determine the best-performing ML model to forecast air pollution in the Greater Cairo Metropolitan Area (GCMA) in Egypt. The authors reported that higher model accuracy was achieved by modifying the support vector regression (SVR) algorithm by changing the weight of target variable based on chance theory but they suffered from long execution run times. Wang et al.<sup>4</sup> developed an unsupervised ML framework for sensor optimization around active operation sites that combines multiple data sources, including oil and gas infrastructure data, historical methane leak rate distribution, topographical data, and meteorological data. The proposed framework achieved an 87.9% success rate in detecting CH<sub>4</sub> leak sources, whereas the baseline model detected 82.8% of sources responsible for fugitive CH<sub>4</sub> emissions. In Travis et al.,<sup>16</sup> an artificial neural network (ANN) was developed using input information as measured, by sonic anemometer wind velocities and CH<sub>4</sub> sensor time series. This allowed the authors to infer the location and release rate of a gas leak. The authors found that the ANN failed to detect very low leak rates and that parameters, such as wind speed and direction, can negatively impact the model's performance. Wang et al.<sup>7</sup> considered the problem of methane leak size classification using a video classification task. This enabled the authors to develop deep learning models to classify videos by leak volume. The authors compared 3 deep

learning algorithms and achieved leak and non-leak detection success rates of nearly 100%.

## Materials and Analysis Pre-requisite

### Dataset

The data used in our study was generated using a comprehensive mesoscale meteorological modeling system, the Regional Atmospheric Modeling System,<sup>17</sup> also referred to as RAMS, which is used by the Savannah River National Laboratory (SRNL) for weather forecasting and airborne dispersion model to simulate toxic release. The model solves the explicit dynamic equations for different meteorological parameters on a three-dimensional grid for a given location and time to simulate atmospheric dynamics, thermodynamics, precipitation, and land surface processes. The RAMS model configuration used in this study is similar to that described in Werth and Buckley,<sup>18</sup> but using a finer grid. We ran the model over a 125 m grid on a  $7.6 \times 7.6$  km domain. The model ran for 6 hours, starting on February 10th, 2022, at 1200 UTC and ending on February 10th, 2022, at 1800 UTC. During the runtime, data was saved every 6 minutes. The model data covers a latitude from  $33.216^\circ\text{N}$  to  $33.284^\circ\text{N}$  and a longitude from  $-81.69^\circ\text{W}$  to  $-81.61^\circ\text{W}$ .

The Hybrid Single-Particle Lagrangian Integrated Trajectory model (HYSPLIT, Stein et al.<sup>19</sup>) is widely used for trajectory mapping and dispersion simulation modeling of atmospheric releases, which require meteorological data as input. Meteorological data collected from the RAMS model were used in a subsequent run of the HYSPLIT model to simulate an airborne tracer's downwind motion and mixing and to predict the tracer concentrations at various locations. The weather and concentration data were organized for each grid location at 6-minute intervals.

The simulation was centered over the Savannah River Site (SRS). The SRS comprises approximately 310 square miles and lies alongside the Savannah river. The landscape is primarily forested with pine trees ranging from 10 to 20 m in height, and industrial facilities are strategically clustered in separate areas connected by roads, which includes multiple buildings of varying sizes. The simulated release point was at  $33.25^\circ\text{N}$  and  $81.65^\circ\text{W}$ . The topography consists of rolling hills, gradually descending from an elevation of 128 m above sea level in the northeast to 30 m above sea level in the southwest. The lowest points were found along the floodplain bordering the river at the southwest boundary, where several on-site creeks drain. During the 6-hour simulation, the wind direction transitions from midway between west and northwest (WNW) to southwest (SW). Assuming a large but plausible release (147 metric tons per hour), our tracer concentration values from the HYSPLIT model were on the order of 0.2 to 2.0 parts per million by volume (ppm-V).

The simulation dataset consists of 301,340 entries with one timing variable (i.e., time), 2 location variables (i.e., latitude

and longitude), and 12 meteorological parameters, such as temperature, relative humidity, pressure, water vapor, turbulent kinetic energy, precipitation rate, sensible heat flux, latent heat flux, west to east wind velocity, south to north wind velocity, vertical wind velocity, and tracer concentration. Figure 1 presents descriptive statistics of the various meteorological parameters obtained from the RAMS model and tracer concentration obtained from the HYSPLIT model.

### Data preprocessing

Among the 301,340 entries in our dataset, only 8,850 entries are associated with  $\text{CH}_4$  leakage (i.e., Tracer concentration  $> 0$ ), whereas it has 292,490 entries with no  $\text{CH}_4$  (i.e., Tracer concentration = 0). Therefore, we used random under-sampling to extract 8,850 entries with no  $\text{CH}_4$  leakage to get a balanced dataset. Our balanced dataset consists of 17,700 entries, including an equal number of entries with  $\text{CH}_4$  leakage and no  $\text{CH}_4$  leakage. Next, we removed the timing and location variables from the balanced dataset, as the ML models should only depend on the meteorological parameters. Moreover, from Figure 1, we see precipitation rate has a constant value of zero for all the entries of the dataset, so we dropped this parameter. Then, we have a cleaned dataset of 17,700 entries with 11 meteorological parameters. Next, we introduced a new binary label Leakage, where leakage equals class 1 if the tracer concentration is greater than zero otherwise to class 0. We removed tracer concentration from the dataset, used leakage as the target binary label, and the 10 meteorological parameters as the input features for the classification binary model.

For the regression model, we only considered entries with tracer concentration  $> 0$ , where tracer concentration served as the target variable, and the 10 meteorological parameters served as the input features. For both classification and regression analyses, we used 4:1 random splitting to generate train and test datasets. Since the different meteorological parameters in our dataset have different ranges of values (as seen in Figure 1) and our target variable for regression, that is, tracer concentration, holds extremely small values compared to the other meteorological parameters. We scaled the parameters in our training and testing datasets for regression analysis based on the equation, scale value =  $(x - \mu) / \sigma$  where  $\mu$  and  $\sigma$  denote the mean and the standard deviation of a given meteorological parameters, respectively. Figure 2 presents all the steps of data preprocessing for a better understanding.

### Ensemble learning models and hyperparameters tuning

Adjustable parameters used during ML model development are called hyperparameters, which regulate how the model trains, prevent overfitting on training data and enhance the

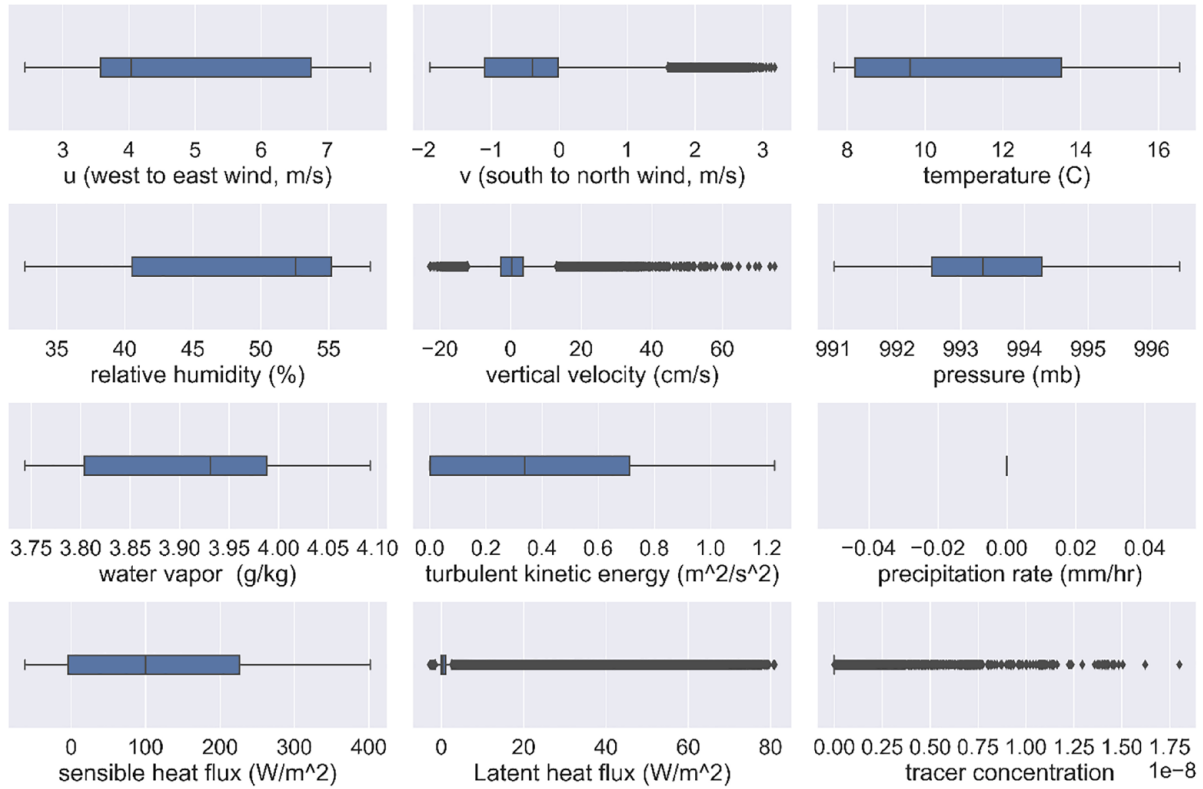


Figure 1. Boxplots of the meteorological parameters obtained from the RAMS model and tracer concentration from the HYSPLIT model.

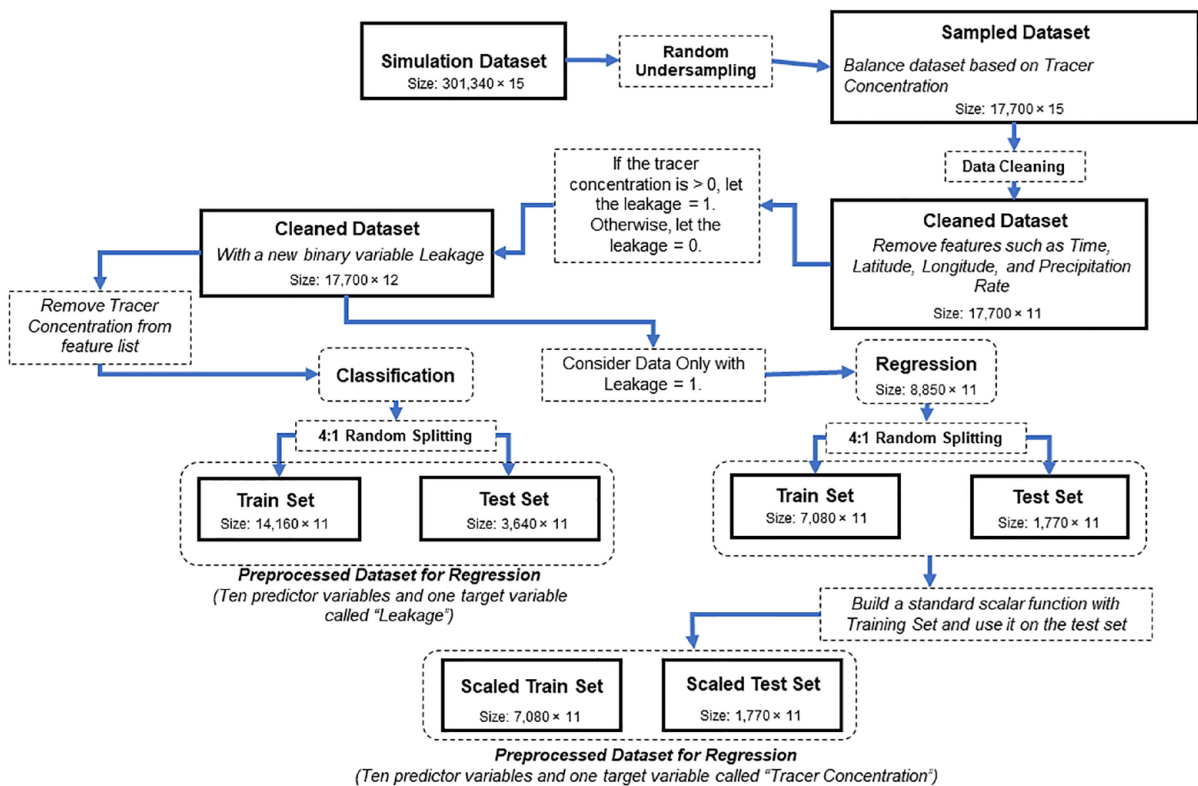


Figure 2. Data preprocessing steps.

model's performance on unknown data. The hyperparameters are tuned for regression and classification tasks to maximize an objective function. For our analysis, we have chosen

accuracy as an objective function for the classification model and  $R^2$  score for the regression models. We have automated our hyperparameter tuning task using Bayesian optimization



and hyperband (BOHB)<sup>20</sup> from the ray tune<sup>21</sup> library to get the optimal set of hyperparameters for our ML models.

*Bayesian optimization and hyperband (BOHB).* It is the state-of-the-art algorithm for hyperparameter optimization that combines the efficiency of hyperband's<sup>22</sup> successive halving strategy for resource allocation with global optimization capability of Bayesian optimization<sup>23</sup> by maintaining a probabilistic model of the objective function based on observed performance. It efficiently navigates the hyperparameter search space iteratively by refining its understanding of promising configurations and allocating resources judiciously.

For our study, we have mainly used 3 types of models (1) tree-based models, (2) gradient boosting models, and (3) K-nearest neighbors.

*Tree-based models.* Among the tree-based models we employed in our research were Extra Trees (ET) and Random Forest (RF), constructed using several decision trees. The maximum depth of the tree (max\_depth), the minimum number of samples needed to split an internal node (min\_samples\_split), the minimum number of samples needed to be at a leaf node (min\_samples\_leaf), and the total number of trees utilized by these models (n\_estimators) are the critical parameters for these models. The criterion (criterion) parameter, which contains options like "gini" for Gini impurity and "entropy" for information gain, specifies the quality metric for node splitting.

*Gradient boosting models.* In our investigation, we employed various gradient boosting models, including the Light Gradient Boosting Model (LGBM), the Extreme Gradient Boosting Model (XGBoost), and the categorical boosting (CatBoost) model. The number of boosting rounds (num\_boost\_round) and learning rate (learning\_rate) are critical hyperparameters for these models.

*K-Nearest Neighbor.* The primary hyperparameters in K-Nearest Neighbor (KNN) used are "weights" which affects how much surrounding data points contribute to predictions.

## Discussion on Methods and Results

RAMS tools are actively used in SRNL to gather meteorological parameters and as input to various airborne dispersion models for detecting toxic gases. The HYSPLIT is a physics-based model widely used in gaseous dispersion modeling. These models encounter limitations like scalability, and computational requirements and often fail to map changes in atmospheric conditions. Furthermore, the HYSPLIT primarily relies on meteorological data; it is more difficult to integrate it with other data sources, like satellite imagery or real-time sensor data, which would limit its ability to adapt to changing atmospheric conditions.

The ML-based ensemble learning models present a viable solution for these shortcomings. The ensemble models are

well-suited for real-time or near-real-time applications because, once trained, they commonly demonstrate lower computing load and inference time. Additionally, the ensemble learning models allow for the smooth integration of many different data sources, offering a more scalable and flexible solution than the gas dispersion models. In addition to their capacity to capture non-linear interactions and manage uncertainty through ensemble aggregation of features, they are useful substitutes for situations involving complicated and dynamic gas dispersion patterns and atmospheric conditions.

In this study, we have used meteorological parameters as inputs to ensemble learning models to detect CH<sub>4</sub> emissions. However, to obtain ground truth for training and testing the models, we have used the output from the HYSPLIT, a gaseous dispersion model.

### *Methane detection using ensemble learning-based classification model*

We formulated the CH<sub>4</sub> detection task as a classification problem by introducing a binary target label Leakage. We used the ensemble learning method to develop and determine the best-performing model for this binary classification problem.<sup>24</sup> The final best-performing model is built upon multiple classifier models using weighted averaging. The underlying classifier models are base layer (L1) models, which were directly trained on the input features (i.e., 10 meteorological parameters). These models include various configurations of the light gradient boosting method (LGBM), extreme gradient boosting method (XGBoost), random forest (RF), extra trees (ET), K-nearest neighbors (KNN), and category boosting (CatBoost). We used the bootstrap aggregating (bagging) ensemble learning technique to train our base layer models using five fold cross-validation. Next, weighted averaging was used to determine the optimum combination of the base layer models, resulting in the best-performing model in the output layer (L2). Our final best-performing classifier model is a weighted average ensemble of 5 base layer models (Figure 3). We used an open-source ML library called AutoGluon<sup>25</sup> developed by Amazon to train all our ensemble models.

For performance evaluation of the classifier models, we used 4 performance metrics, (i) accuracy (ii) F1-Score, (iii) Mathew's Correlation Coefficient (MCC), and (iv) area under the receiver operating characteristics curve (AUC ROC). The performance metrics were determined using the following equations,

$$\text{ACCURACY} = \frac{TP + TN}{TP + FP + TN + FN}$$

$$\text{F1} = \frac{TP}{TP + (FP + FN) / 2}$$

$$\text{MCC} = \frac{((TP \times TN) - (FP \times FN))}{\sqrt{(TP + FP) \times (TP + FN) \times (TN + FP) \times (TN + FN)}}$$

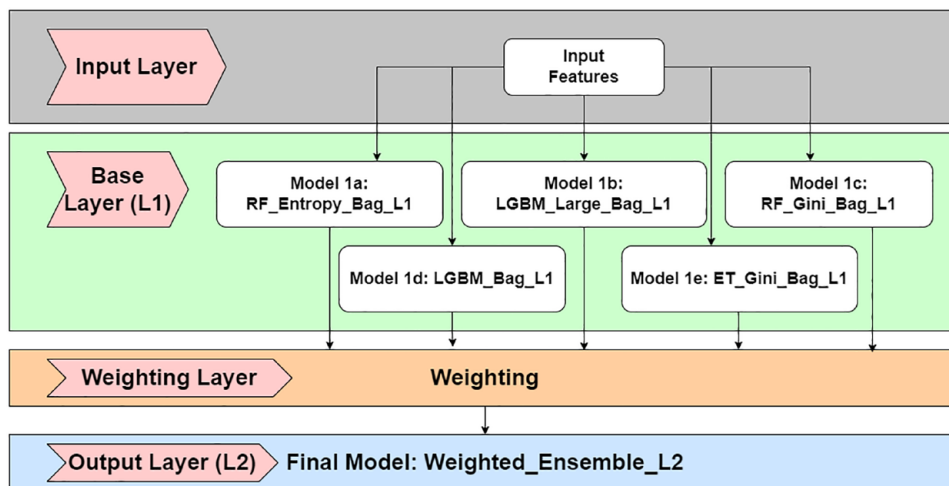


**Figure 3.** Steps and the weaker classifier models involved in generating the best-performing classifier model using ensemble learning.

**Table 1.** Performance of classification models on the test set.

MODEL	PERFORMANCE METRIC					
	ACCURACY (%)	F1-SCORE	AUC_ROC	PRECISION	RECALL	MCC
WeightedEnsemble_L2	97.2	0.972	0.995	0.949	0.997	0.945
LGBM_Large_BAG_L1	97.2	0.972	0.993	0.950	0.996	0.945
LGBM_BAG_L1	97.1	0.971	0.993	0.947	0.997	0.943
XGBoost_BAG_L1	96.9	0.970	0.993	0.944	0.997	0.939
ET_Gini_BAG_L1	96.7	0.968	0.995	0.940	0.997	0.936
RF_Gini_BAG_L1	96.7	0.968	0.995	0.943	0.994	0.935
LGBM_XT_BAG_L1	96.7	0.967	0.991	0.941	0.995	0.935
RF_Entropy_BAG_L1	96.6	0.967	0.995	0.942	0.994	0.934
ET_Entropy_BAG_L1	96.6	0.967	0.995	0.938	0.997	0.934
CatBoost_BAG_L1	96.4	0.965	0.991	0.935	0.997	0.930
KNN_Distance_BAG_L1	87.6	0.885	0.933	0.820	0.961	0.763
KNN_Uniform_BAG_L1	87.0	0.879	0.927	0.816	0.952	0.750

$$\text{AUC ROC} = \int_0^1 \frac{TP}{TP + TN} d\left(\frac{FP}{FP + FN}\right)$$

where, TP, TN, FP, and FN denote true positive, true negative, false positive, and false negative, respectively. Table 1 presents the performance of our base layer models and the final best-performing classifier model. The models presented in Table 1 show the performance of all the models used in our study. Our final ensemble model achieved an accuracy of 97.2% on the test dataset and the other performance metrics, such as F1 score, Precision, Recall, MCC, and AUC ROC are 0.972, 0.949, 0.997, 0.945, and 0.995. Hyperparameters for our best model i.e. Weighted\_Ensemble\_L2 and all the contributing base models are presented in Table 2.

#### *Methane intensity prediction using ensemble learning-based regression model*

Our CH<sub>4</sub> intensity prediction task aims to predict the intensity of CH<sub>4</sub> (i.e., Tracer concentration of CH<sub>4</sub>) at any given location once our final classifier model detects the presence of CH<sub>4</sub> at that location. As mentioned before, our regression models for CH<sub>4</sub> intensity prediction were trained on 10 meteorological parameters, and all these features were standardized before fitting into multiple models for regression. For the performance evaluation of our regression models, we used the model with the best  $R^2$  value on the validation set. Later, we validated our results with  $R^2$  score, Mean Square Error (MSE), and Root Mean Square Error (RMSE) score on the test data using the following equation,

**Table 2.** Hyperparameter settings of the final model for classification in this study.

LAYER	MODEL	HYPERPARAMETER
Output Layer (L2)	WeightedEnsemble_L2	Ensemble Size: 27, RF_Entropy_BAG_L1, RF_Gini_BAG_L1, LGBM_Large_BAG_L1, ET_Gini_BAG_L1, LGBM_BAG_L1
Base Layer (L1)	LGBM_Large_BAG_L1	Learning rate: 0.03, Number of Leaves: 128, Feature fraction: 0.9, Minimum data in leaf: 5, Number of boost round: 508
	LGBM_BAG_L1	Learning rate: 0.05, Number of boost round: 900
	ET_Gini_BAG_L1	Number of Estimators: 300, Maximum Leaf Nodes: 15000, Criterion: Gini
	RF_Gini_BAG_L1	Number of estimators: 300, Maximum leaf nodes: 15000, Criterion: Gini
	RF_Entropy_BAG_L1	Number of estimators: 300, Maximum leaf nodes: 15000, Criterion: Entropy

$$R^2 = 1 - \frac{SSR}{SST}$$

$$MSE = \frac{1}{N} \sum_{i=1}^N SST$$

$$RMSE = \sqrt{MSE} = \sqrt{\frac{1}{N} \sum_{i=1}^N SST}$$

where, SSR refers to the sum of squared differences (residuals) between the actual values and the predicted values, SST refers to the sum of squared distances of the actual values from the mean of the actual values (totals), and N equals to the number of samples.

Our regression-based ensemble learning models were generated in 2 stages. In the first stage, our base layer (L1) models were trained directly on the 10 meteorological parameters to predict the tracer concentration. These models include various configurations of LGBM, XGBoost, RF, ET, and KNN. In the second stage, we have the stacker layer (L2) models that were developed considering the 10 meteorological parameters as well as the regression outputs from base layer (L1) regression models as input features to better predict the intensity of CH<sub>4</sub>. Finally, weighted averaging was used to determine the optimum combination of stacker layer (L2) models that results in the best-performing model in the output layer (L3). Table 3 presents the performance of all our regression models from the base layer (L1) and stacker layer (L2) selected based on the highest R<sup>2</sup> scores on the validation and test set. Our final best-performing regression model is a weighted averaged ensemble model of 4 stacker layer models 2a to 2d (as shown in Figure 4), and it achieved an R<sup>2</sup> score of 0.812 on the validation set. Using the same model for the test set we received an R<sup>2</sup> of 0.858 which is higher than other models. We also calculated mean squared error (MSE) of 0.148 and Root Mean Squared Error of 0.385 which is lower than all other models with similar R<sup>2</sup> values (as shown in Table 3). Table 4 provides the hyperparameter settings for all the models that were involved in generating our final best-performing regression model (i.e., Weighted\_Ensemble\_L3).

Figure 5 shows actual and predicted tracer concentrations from the best ensemble model at different locations using latitude and longitude along the *x* and *y* axes. We have presented the results for 3 different time periods. Data from these 3 time periods were not used during the machine learning training.

#### *ML-based methane detection in a distributed system*

The ML models used in this research to autonomously detect fugitive CH<sub>4</sub> emissions from environmental data and predict the corresponding intensity in the detected areas, have been trained and validated using local computers in this study. However, such ML models can be extended into a distributed ML-based CH<sub>4</sub> environmental emission detection system by deploying multiple environmental sensing modalities with each modalities possessing its own computational processing units (CPU).

Figure 6 displays the framework of a fugitive CH<sub>4</sub> environmental emission detection Cyber-Physical System (CPS) where data storage, execution, optimization, and retraining of ML models will be accomplished by using cloud-based technology to ensure efficient real-time system operation. Additionally, real-time synchronous coordination of environmental data acquired by multiple sensor edges will achieve optimal system operation. The environmental emissions detection ML models will filter and calibrate meteorological information gathered from EPA ground stations as the UAVs monitor geographical areas of interest to keep false alarms minimal. As new environmental conditions are used to train the models, this distributed ML-based fugitive CH<sub>4</sub> environmental emissions detection CPS will achieve large-scale autonomous detection of CH<sub>4</sub>.

#### **Conclusions**

In this study, we developed an ensemble learning-based detection and intensity prediction system for environmental CH<sub>4</sub> emission. The dataset used in our analysis is a simulated dataset that was provided by the Savannah River National Laboratory. We formulated the CH<sub>4</sub> detection task as a classification problem and the CH<sub>4</sub> intensity prediction task as a regression problem. For both tasks, we used the ensemble learning method to

**Table 3.** Performance of regression models on test set.

MODEL	PERFORMANCE METRIC			
	ROOT MEAN SQUARED ERROR (RMSE)	MEAN SQUARED ERROR (MSE)	TESTING SET $R^2$	VALIDATION SET $R^2$
WeightedEnsemble_L5	0.388	0.150	0.856	0.804
CatBoost_BAG_L4	0.382	0.146	0.860	0.800
XGBoost_BAG_L4	0.387	0.150	0.856	0.779
LGBM_XT_BAG_L4	0.392	0.153	0.853	0.780
ET_MSE_BAG_L4	0.394	0.156	0.851	0.797
RF_MSE_BAG_L4	0.397	0.158	0.848	0.784
LGBM_BAG_L4	0.398	0.158	0.848	0.791
LGBM_Large_BAG_L4	0.408	0.167	0.840	0.790
WeightedEnsemble_L4	0.375	0.140	0.865	0.803
XGBoost_BAG_L3	0.366	0.134	0.871	0.783
RF_MSE_BAG_L3	0.369	0.136	0.869	0.791
CatBoost_BAG_L3	0.377	0.142	0.864	0.801
ET_MSE_BAG_L3	0.378	0.143	0.863	0.798
LGBM_XT_BAG_L3	0.384	0.147	0.858	0.785
LGBM_BAG_L3	0.385	0.148	0.858	0.781
LGBM_Large_BAG_L3	0.397	0.158	0.848	0.770
WeightedEnsemble_L3	0.385	0.148	0.858	0.812
XGBoost_BAG_L2	0.376	0.142	0.864	0.784
RF_MSE_BAG_L2	0.381	0.145	0.860	0.801
ET_MSE_BAG_L2	0.383	0.147	0.859	0.807
LGBM_Large_BAG_L2	0.386	0.149	0.857	0.787
CatBoost_BAG_L2	0.390	0.152	0.854	0.808
LGBM_XT_BAG_L2	0.400	0.160	0.847	0.788
LGBM_BAG_L2	0.405	0.164	0.843	0.799
WeightedEnsemble_L2	0.437	0.191	0.816	0.792
CatBoost_BAG_L1	0.417	0.174	0.833	0.770
LGBM_Large_BAG_L1	0.447	0.200	0.808	0.774
XGBoost_BAG_L1	0.452	0.204	0.804	0.762
ET_MSE_BAG_L1	0.459	0.211	0.798	0.766
LGBM_BAG_L1	0.482	0.232	0.777	0.739
RF_MSE_BAG_L1	0.494	0.244	0.766	0.771
LGBM_XT_BAG_L1	0.502	0.252	0.758	0.720
KNN_Distance_BAG_L1	0.607	0.368	0.647	0.577
KNN_Uniform_BAG_L1	0.610	0.372	0.643	0.571



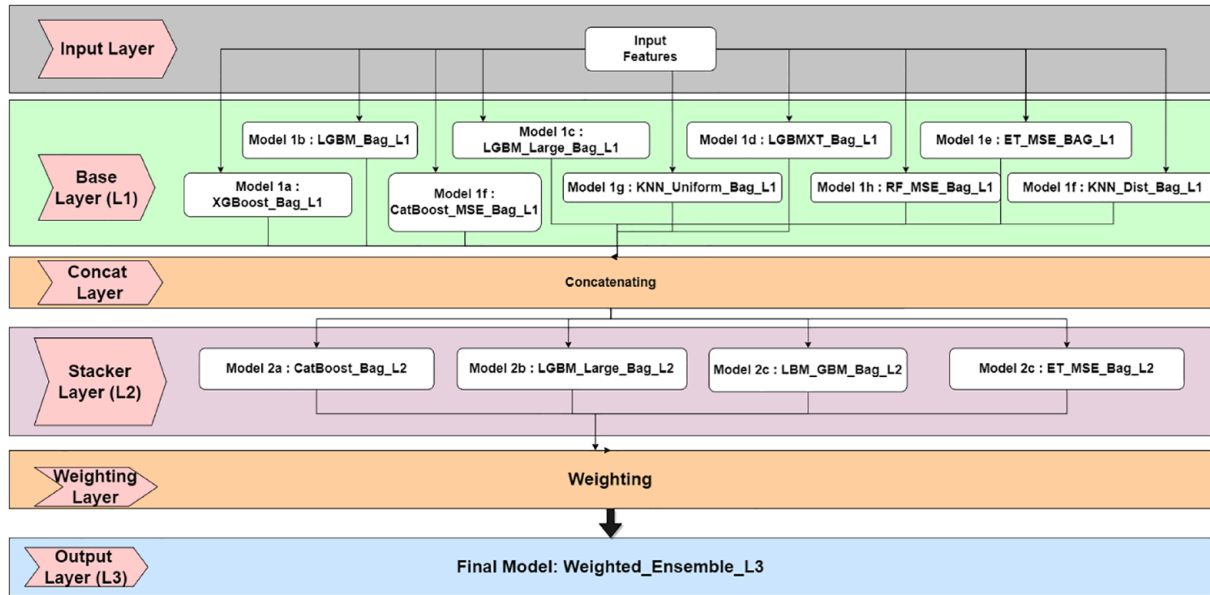


Figure 4. Steps and weaker regression models involved in generating the best-performing regression models using ensemble learning.

Table 4. Hyperparameter settings of the final model for regression in this study.

LAYER	MODEL	NUMBER OF FEATURES	HYPERPARAMETER
Output Layer (L3)	WeightedEnsemble_L3	4	Ensemble Size: 100, LGBM_BAG_L2, CatBoost_BAG_L2, ET_MSE_BAG_L2, LGBM_Large_BAG_L2
Stacker Layer (L2)	LGBM_BAG_L2	19	Learning rate: 0.05, Number of boost rounds: 58
	CatBoost_BAG_L2	19	Iterations: 714, Learning rate: 0.05, Evaluation metric: R2
	ET_MSE_BAG_L2	19	Number of estimators: 300, Maximum leaf nodes: 15000, Criterion: Squared error
	LGBM_Large_BAG_L2	19	Learning rate: 0.03, Number of leaves: 128, Feature fraction: 0.9, Minimum data in Leaf: 5, Number of boost rounds: 172
Base Layer (L1)	RF_MSE_BAG_L1	10	Number of estimators: 300, Maximum Leaf Nodes: 15000, Criterion: Squared Error
	LGBM_XT_BAG_L1	10	Learning Rate: 0.05, Extra Trees: True, Number of Boost Rounds: 3668
	ET_MSE_BAG_L1	10	Number of Estimators: 300, Maximum leaf nodes: 15000, Criterion: Squared error
	KNN_Uniform_BAG_L1	10	Weights: Uniform
	CatBoost_BAG_L1	10	Iterations: 9226, Learning rate: 0.05, Evaluation metric: R <sup>2</sup>
	LGBM_Large_BAG_L1	10	Learning rate: 0.03, Number of leaves: 128, Feature fraction: 0.9, Minimum data in Leaf: 5, Number of boost rounds: 489
	KNN_Distance_BAG_L1	10	Weights: Distance
LGBM_BAG_L1	10	Learning rate: 0.05, Number of boost rounds: 602	

generate ML models built upon several weaker ML models from base and stacker layers to yield better classification and regression performance. Our best-performing classifier model achieved an accuracy of 97.2% with an F1 score of 0.974, an MCC of 0.945, and an AUC ROC of 0.995 on the test dataset,

whereas our best-performing regression model achieved an R<sup>2</sup> score of 0.858. One limitation of this study is that we utilized simulation data for developing our ensemble models. In the future, we will assess the performance of our model using real-world data to further validate the performance of our models in

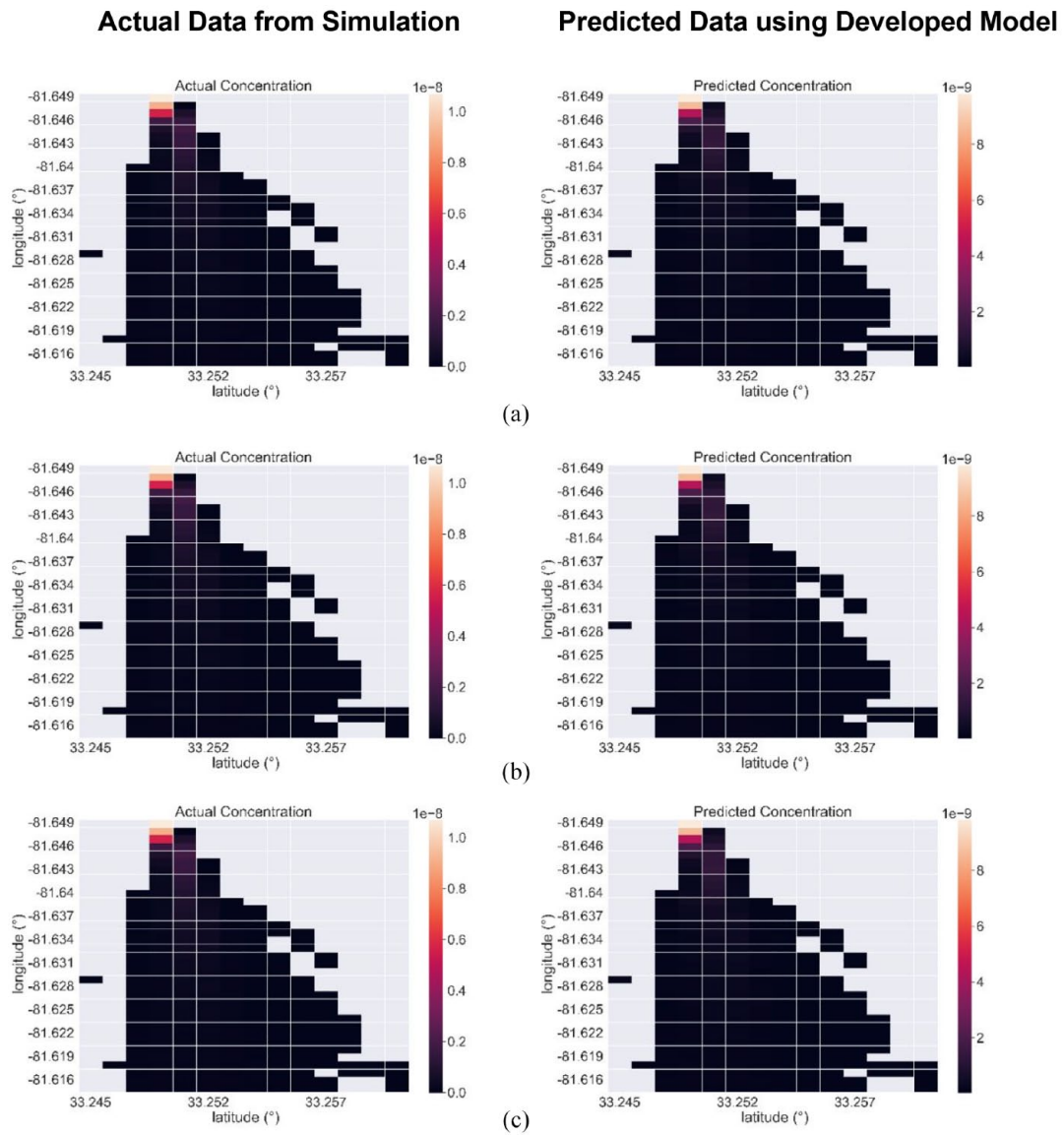


Figure 5. Actual and predicted tracer concentration at: (a) 5.00 PM, (b) 5.12 PM, and (c) 5.24 PM.

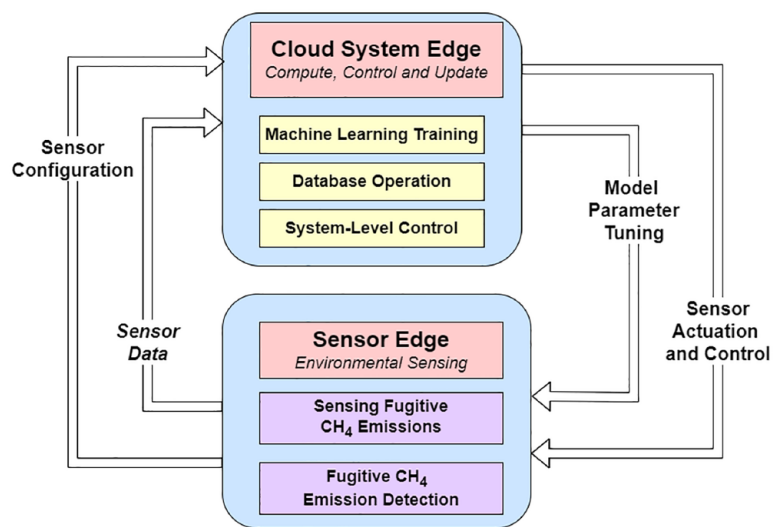


Figure 6. Fugitive CH<sub>4</sub> environmental sensing CPS.

the detection and intensity prediction of environmental CH<sub>4</sub> emissions.

### Future Scope

Gas dispersion models are computationally expensive and not suitable for real-time gas detection. This paper was our first step toward a scalable ML-based detection method using meteorological parameters and comparing it with dispersion models like HYSPLIT. In our next step, we will extend this research to gather meteorological data from real-world sensors on the edge to test and validate our ensemble learning models for detection.

One of the limitations of our model is that it is dependent on meteorological parameters only. In our next step, we plan to reduce the dependency on meteorological data by using and collecting CH<sub>4</sub> sensor data using a drone and generating sensor-specific ensemble learning models that can be deployed in the cloud. Multiple ML models for different data sources can work in parallel to better map a geographical area for CH<sub>4</sub> emissions.

### Author Contributions

RM: Conceptualization, Methodology, Implementation, Formal Analysis, Writing-original draft, Writing-review & editing. JP: Implementation, Formal Analysis, Writing-original draft. MSS: Methodology, Writing-original draft, Writing-review & editing. DW: Data Curation, Validation, Writing-original draft, Writing-review & editing. GC: Resources, Project administration, Funding acquisition, Writing-review. AG: Validation, Writing-original draft, Writing-review & editing. SMK: Conceptualization, Writing-original draft, Supervision. SD: Supervision, Funding acquisition. MC: Conceptualization, Supervision, Funding acquisition, Writing-original draft, Writing-review & editing.

### REFERENCES

- U.S. Energy information administration - EIA - independent statistics and analysis. John Conti, Paul Holtberg, Perry Lindstrom. Published in March 31, 2011. Accessed November 28, 2023 [Online]. [https://www.eia.gov/environment/emissions/ghg\\_report/ghg\\_methane.php](https://www.eia.gov/environment/emissions/ghg_report/ghg_methane.php)
- N. US Department of Commerce. Global monitoring laboratory - carbon cycle greenhouse gases. Accessed December 04, 2023 [Online]. Updated October, 2023. <https://gml.noaa.gov/ccgg/ghgpower/>
- O. US EPA. Understanding global warming potentials. Accessed December 04, 2023 [Online]. Last Updated April, 2023. <https://www.epa.gov/ghgemissions/understanding-global-warming-potentials>
- Wang S, Malva S, Nunes L, et al. Unsupervised machine learning framework for sensor placement optimization: analyzing methane leaks. Presented at: NeurIPS 2021 Workshop on Tackling Climate Change with Machine Learning, 2021.
- O. US EPA. Overview of greenhouse gases. Accessed December 04, 2023 [Online]. Last Updated October, 2023. <https://www.epa.gov/ghgemissions/overview-greenhouse-gases>
- General pipeline FAQs | PHMSA. Accessed December 04, 2023 [Online]. Office of Pipeline Safety U.S. Department of Transportation, Pipeline and Hazardous Materials Safety Administration. Last Updated November, 2018. [https://www.phmsa.dot.gov/faqs/general-pipeline-faqs#:~:text=Liquid%20petroleum%20\(oil\)%20pipelines%20transport,%2C%20jet%20fuels%2C%20and%20kerosene.00](https://www.phmsa.dot.gov/faqs/general-pipeline-faqs#:~:text=Liquid%20petroleum%20(oil)%20pipelines%20transport,%2C%20jet%20fuels%2C%20and%20kerosene.00)
- Wang J, Ji J, Ravikumar AP, et al. VideoGasNet: Deep learning for natural gas methane leak classification using an infrared camera. *Energy*. 2022;238:121516. Accessed December 04, 2023 [Online]. <https://www.sciencedirect.com/science/article/pii/S0360544221017643?via%3DIihub>
- Hino M, Benami E, Brooks N. Machine learning for environmental monitoring. *Nat Sustain*. 2018;1:583-588.
- Sun S, Ma L, Li Z. Methane emission estimation of oil and gas Sector: A review of measurement technologies, Data Analysis Methods and uncertainty estimation. *Sustainability*. 2021;13:7-9. doi:10.3390/su132413895
- Bu F, Liu Y, Wang Z, et al. Analysis of natural gas leakage diffusion characteristics and prediction of invasion distance in utility tunnels. *J Nat Gas Sci Eng*. 2021;96:1-3.
- Fleming NA, Morais TA, Mayer KU, Ryan MC. Spatiotemporal variability of fugitive gas migration emissions around a petroleum well. *Atmos Pollut Res*. 2021;12:3-6.
- Bezyk Y, Sówka I, Górka M, Nęcki J. Spatial and temporal patterns of methane uptake in the urban environment. *Urban Clim*. 2022;41:3-6.
- Okorn K, Jimenez A, Collier-Oxandale A, Johnston J, Hannigan M. Characterizing methane and total non-methane hydrocarbon levels in Los Angeles communities with oil and gas facilities using air quality monitors. *Sci Total Environ*. 2021;777:2-6.
- Hähnel P, Mareček J, Monteil J, O'Donncha F. Using deep learning to extend the range of air pollution monitoring and forecasting. *J Comput Phys*. 2020; 408:5-9.
- Eldakhly NM, Aboul-Ela M, Abdalla A. A novel approach of weighted support vector machine with applied chance theory for forecasting air pollution phenomenon in Egypt. *Int J Comput Intell Appl*. 2018;17:1850001.
- Travis B, Dubey M, Sauer J. Neural networks to locate and quantify fugitive natural gas leaks for a MIR detection system. *Atmos Environ*. 2020;8:2-7.
- Pielke RA, Cotton WR, Walko RL, et al. A comprehensive meteorological modeling system?—RAMS. *Meteorol Atmos Phys*. 1992;49:69-91.
- Werth D, Buckley R. The application of a genetic algorithm to the optimization of a mesoscale model for emergency response. *J Appl Meteorol Climatol*. 2022;61:329-343.
- Stein AF, Draxler RR, Rolph GD, et al. NOAA's HYSPLIT atmospheric transport and dispersion modeling system *Bull Am Meteorol Soc*. 2015;96 (12):2059-2077.
- Falkner S, Klein A, Hutter F. BOHB: robust and efficient hyperparameter optimization at scale. arXiv, July 04, 2018. doi: 10.48550/arXiv.1807.01774
- Liaw R, Liang E, Nishihara R, et al. Tune: A research platform for distributed model selection and training. arXiv preprint arXiv. 1807.05118. 2018.
- Li L, Jamieson K, DeSalvo G, Rostamizadeh A, Talwalkar A. Hyperband: a novel bandit-based approach to hyperparameter optimization. arXiv.org, June 18, 2018. Accessed December 06, 2023 [Online]. <https://arxiv.org/abs/1603.06560v4>
- Klein A, Falkner S, Bartels S, Hennig P, Hutter F. Fast Bayesian optimization of machine learning hyperparameters on large datasets. arXiv, March 07, 2017. doi: 10.48550/arXiv.1605.07079
- Pollard J. Development and Evaluation of Machine Learning Models for Fugitive Methane Detection and Intensity Prediction. *All Theses*. 2023;4065. [https://tigerprints.clemson.edu/all\\_theses/4065](https://tigerprints.clemson.edu/all_theses/4065)
- Erickson N, Mueller J, Shirkov A, et al. Autogluon-tabular: Robust and accurate automl for structured data. arXiv preprint arXiv:2003.06505. 2020.